Paper: ASAT-15-195-PP

15th International Conference on
AEROSPACE SCIENCES & AVIATION TECHNOLOGY,
ASAT - 15 – May 28 - 30, 2013, Email: asat@mtc.edu.eg ,
Military Technical College, Kobry Elkobbah, Cairo, Egypt,
Tel: +(202) 24025292 –24036138, Fax: +(202) 22621908

The Effect of Tangential Swirl Angle on NO_X Formation in a Non-Premixed LPG/Air Flame

M. A. Abdel-Al*, M. A. Yehia†, M. R. Taha†, T. W. Abou-Arab†

Abstract: In the present study the effect of tangential swirl angle on NO_x formation in non premixed liquefied petro gas (LPG) – air flame is examined. The liquefied petrol gas used (LPG) contains of 50% Propane and 50% Butane. A new injection swirl ratio has been introduced for the new Circumferential Arranged Air and Fuel Burner (CAFB) burner namely the injection swirl number (ISN), ISN = tan θ, where θ is the injection angle. The injection swirl number (ISN) used is 0, 0.27, 0.57, 1 and 1.73 which corresponding to the injection angles 0, 15, 30, 45 and 60 degree respectively. An empirical correlation has been derived for the new CAFB burner flame length as a function of the new derived (ISN). The experiments are conducted in an ax symmetric cylindrical combustion chamber for a range of equivalence ratio and swirl angle. The numerical simulations are carried out with the CFD code, Fluent Ansys 6.3. The turbulence k-ε model is employed. Both predictions and experiments show that as the swirl number increase, the temperature and the thermal NO_x first slightly increase and then strongly decrease at the exit of the combustion chamber. An empirical correlation has been derived for the new CAFB burner. Numerical simulations by Fluent Ansys 6.3 were able to obtain reasonable agreement with the experimental results.

Keywords: Burner–Swirl–confined/free diffusion flame–flame length–NO_x–Injection angle

1. Introduction

Swirl combustion is widely found in various thermal power engineering devices, including furnaces, boilers and gas turbine engines [1,2]. Swirling flows have been studied for decades, with detailed descriptions in the work of [3-5]. It was found recently that swirl might influence not only combustion characteristics but also NO_x formation [6]. Swirl is an implement for steady flame and heat transfer control and increased combustion efficiency [7,8]. To meet these requirements, many types of swirl burners were developed, which employ complicated swirl gas/particle flow to ensure their performance [9]. For achieving low NO_x emission as well, swirl combustion has to be integrated with other combustion techniques such as staged combustion, flue gas recirculation (FGR), reburning, and low oxygen combustion [10]. Some researchers reported an increase in NO_x formation with increasing swirl number [6], and the others reported a decrease in NO_x formation with increasing swirl number [11].

The effect of swirl on NO_x formation is a complex phenomenon. The change of swirl number will affect the flow field, including the location and size of the recirculation zone, the flame temperature, species concentration distribution, and turbulence intensity.

* Egyptian Armed Forces, Egypt.
† Prof. of Mechanical Power Engineering, Faculty of Engineering, Cairo University, Egypt.

All these changes will affect NO_x formation, but it is unclear which one dominates [6]. For numerical simulation, most authors use the assumed-PDF turbulence- chemistry model to simulate NO_x formation in turbulent flows [12]. In this paper, the experimental and numerical studies on the effect of swirl number on NO_x formation in propane/air turbulent swirling combustion have been investigated. The standard k – ε model is applied to simulate turbulence flow.

The k – ε model is a two equation eddy viscosity model, which solves for turbulent kinetic energy (k) and its dissipation rate (ε). Probability density function (PDF) is used to model turbulent combustion. The application of a tangential velocity component to the flow, gives the flow a rotating component, represented by the non-dimensional swirl number (S) defined as the ratio of the tangential momentum flux to axial momentum flux, as [13].

$$S = \int_0^R \rho U W r^2 dr \,/\, R_{in} \int_0^R \rho U^2 r dr \qquad (1)$$

Here, R denotes the swirler radius. The NO_x postprocessor is used to predict NO_x emissions.

2. Numerical Simulation

The simulation equations in cylindrical coordinate based on the continuity, momentum and energy can be expressed in the following general forms [14].

Continuity equation:

$$\frac{\partial}{\partial x_i}(\rho u_i + \overline{\rho' u_i'}) = 0 \qquad (2)$$

Conservation equations:

$$(\rho u_j + \overline{\rho' u_j'})\frac{\partial \phi_i}{\partial x_i} + \frac{\partial}{\partial x_j}\left(\rho \overline{u_j' \phi_i'} + u_j \overline{\rho \phi_i} + \overline{\rho u_j \phi_i}\right) = \frac{\partial}{\partial x_j}\left(\Gamma_\phi \frac{\partial \phi}{\partial x_j}\right) + S_\phi \qquad (3)$$

Where r the fluid density, uj is the velocity component along the coordinate Direction xj, F is the dependent variable which can be mass, velocity, and enthalpy. GF is the diffusion coefficient and SF is the source term. Figure 1 displays the geometric model of the new circumferential arranged fuel and air burner, namely CAFB.

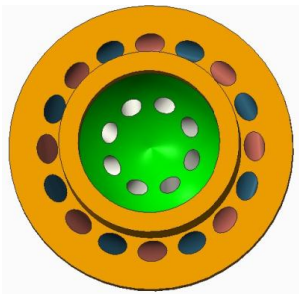

Fig. 1 Geometric model of the new burner

The CFD code Fluent package [15] is applied to simulate a 3D, steady state and axisymmetric geometry. Propane is used as fuel. Figure 2 demonstrates grids of mesh having about 545161 cells.

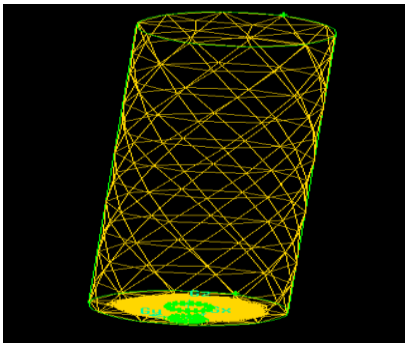

Fig. 2 Preprocessing mesh generation

Fuel and air inlet temperatures are 300 K and pressure is 1 atm. Air inlet velocity is 5 m/s and the wall temperature in simulations is kept at 750 K.

3. Experimental

The experimental setup, including the test section, the air and fuel supply systems, and the measurement system, is shown in Fig 3. The test section is a combustor made of a hollow steel tube.

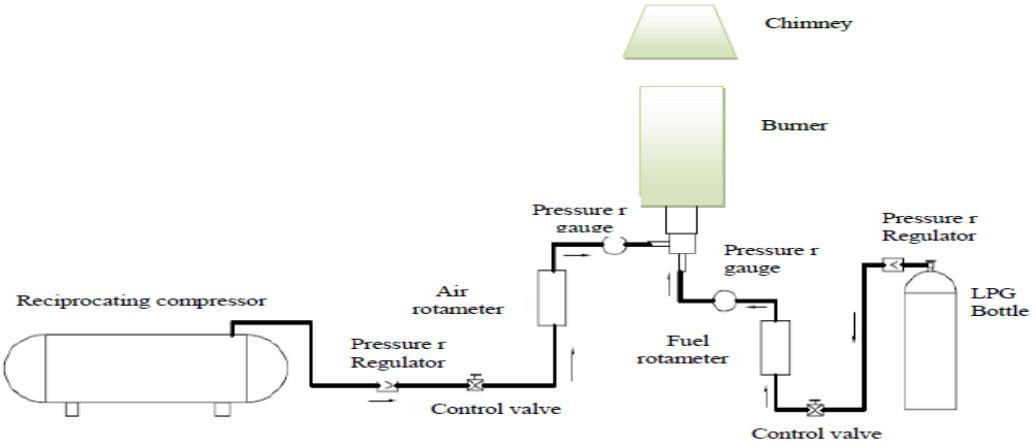

Fig. 3 Experimental setup

The combustor length is 750 mm and its inner diameter is 300 mm. The combustor is insulated with glass fiber of 15mm thickness. The conceptual burner design is to dividing the fuel and air admission ports into 16 holes each with 2.4 mm inner diameter. The fuel and air holes are circumferentially arranged alternatively to increase the fuel to air interaction due to the near distance between the fuel and air streams. The main reason of the improvement of fuel/air interaction is in the smart design in the CAFB burner nozzle, in which each fuel stream is embedded between two air streams, and vice versa such that each air stream is localized between two main fuel streams, and finally the two air and fuel streams are rotated with each others. It means a higher volume to surface ratio for the fuel and the oxidizer, which increases the shear layers acting as a rapid mixing mechanism. the burner outwards flow rotates in a tangential injection bore angles. For parametric study and optimization, these angles varied to covering the entire available tangential span. The burner holes injection angles exhibits at 0, 15, 30, 45 and 60 degree Stability occurs mainly due to the IRZ by the recirculation flow process. A schematic of the design of the CAFB diffusion flame burner is shown in figure 4.

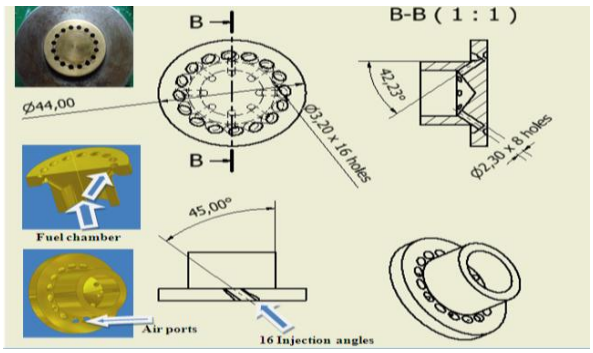

Fig. 4 Schematic of the design of the new burner

The sixteen (eight to the each) ports are arranged alternatively in a circular array with an angular distance of 22.5º and the central distance is 11.5 mm to the head center line. The thickness of the burner head is 5 mm. The even air jets are directly connected to the air supply which passes through the burner tube. The odd fuel jets accumulate in the fuel chamber to equalize the flow from the fuel supply by placing layers of grids in the chamber. The grid layers are to ensure that the flow from each of the fuel and air ports is equal as shown in Figure 5.

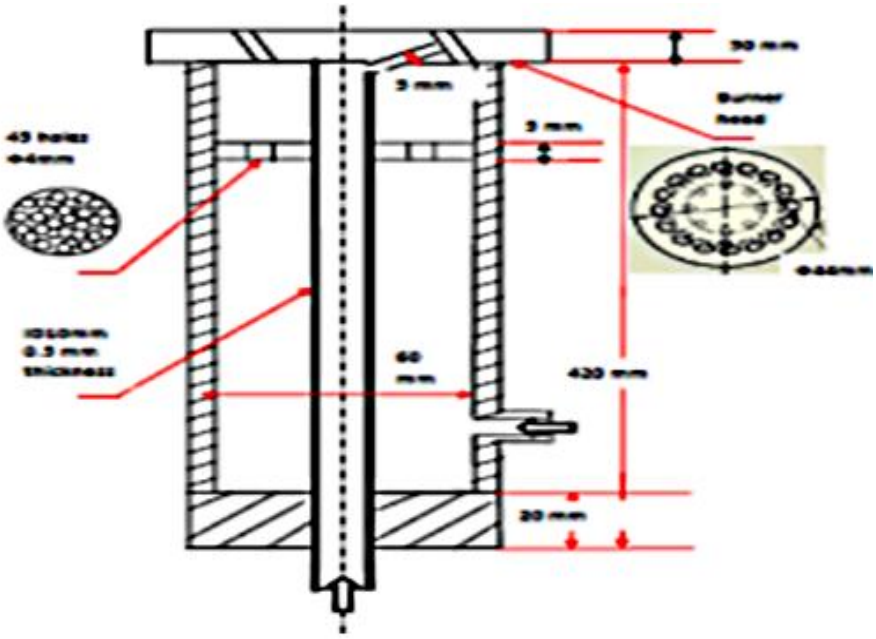

Fig. 5 Burner design

There are three reasons for designing this burner. Firstly, the circumferentially alternated Air and Fuel Burner (CAFB) burner arrangement substantially increases the air and fuel contact surface area by breaking down the annular fuel stream and the central air jet into individual smaller streams. Secondly, the Circumferentially alternated Air and Fuel Burner (CAFB) burner arrangement provides extra fuel jet to fuel jet interaction which enhances the induced turbulence, entrainment effect and air/fuel mixing performance as shown schematically in figure 6.

The third reason is to change of the air and fuel injection angles from (0º, 15º, 30, 45º) up to 60º tangent to the burner head centerline to increasing the swirling effects. This will help to study the effect of injection swirling on emissions and combustion process. In additions, these new design.

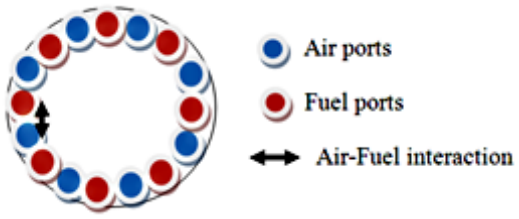

Fig. 6 Effect on fuel jet to air jet interaction

may enables this type of burner to operates under a highly stability limit in free and confined conditions as it will be explained with the aid of obtained experimental data.
The species concentrations were measured using a IMR-2800A gas analyzer. Fuel and air mass flow rate was measured using a Dwyer rotameter. The swirl number is defined as [16]:

$$S = \frac{2\tan\theta}{3}\frac{1-\sigma_r^3}{1-\sigma_r^2} \qquad (4)$$

Where θ is the injection angle and σr is the ratio of swirler inner diameter to outer diameter. The injection angles used in experiments are: 0, 15, 30, 45, and 60 degrees that swirlers show in Fig 7. The injection ports is 2.5 mm in diameter, so, the swirl numbers are 0, 0.27, 0.58, 1 and 1.73, respectively are deduced from equation (4) as flollows:

$$S = \frac{G_{ang}}{R_b G'_x} = \frac{\int_0^\infty \rho U W r^2 dr}{R_b \int_0^\infty \rho (U^2 - \frac{1}{2}W^2) r dr}$$

Where Gang is the angular momentum in the swirled section and G'x is the linear momentum flux through the unswirled center core and the swirled annulus. This terms can be calculated by integrating the mean axial, U, and the mean swirl, W, velocity components across the burner exit. With the assumption that the distribution of the axial flow remains flat, and U and W at the burner exit are kinematically related to the blade angle as tan α = U/W , the axial flux of angular momentum in the annular section is then written as follows:

$$G_{ang} = 2\pi\rho \int_{R_c}^{R_b} U_a (U_a \tan\alpha) r^2 dr = 2\pi\rho U_a^2 \tan\alpha \left(\frac{R_b^3 - R_c^3}{3} \right)$$

Here, Ua is a mean axial velocity supplied through the swirl annulus. By assuming flat axial velocity distribution, the linear momentum flux from the two regions of the burner is then calculated as follows:

$$G_x = 2\pi\rho \int_{R_c}^{R_b} U_a^2 r dr + 2\pi\rho \int_0^{R_c} U_c^2 r dr = \pi\left[\rho U_a^2 (R_b^2 - R_c^2) + \rho U_c^2 R_c^2\right]$$

Where Uc is a mean axial velocity through the center core. With Equation (1-9) as defined, the geometric swirl number for the vane swirl burner is then:

$$S = \frac{\frac{2}{3}\tan\alpha(1-R^3)}{1-R^2+\frac{U_c^2}{U_a^2}R^2} = \frac{2}{3}\tan\alpha \frac{1-R^3}{1-R^2+[m^2(1/R^2-1)^2]R^2}$$

Where: α …..the injection angle

R….ratio of the center channel radius (Rc) to injector radius (Ri)
m….mass flux ratio (between mass flux through center channel (mc) and mass flux through swirl annulus (ms))
For the new burner (CAFB):
a- Channel radius is the injection radius (R≡1), let R=0.9 for simplicity.
b- Channel in annulus, so the center channel is the swirl annulus. i.e m=1.
Substitute in Equation (1-10) we got the new formula for the injection swirl number for the new burner (CAFB)..

$$S = 2/3 \tan \alpha \, (3/2)$$
$$ISN = \tan \alpha$$

Where α is the injection angle tangent to the burner surface, and ISN is the new correlation for injection swirl number for the multi fuel jet in this case (CAFB).

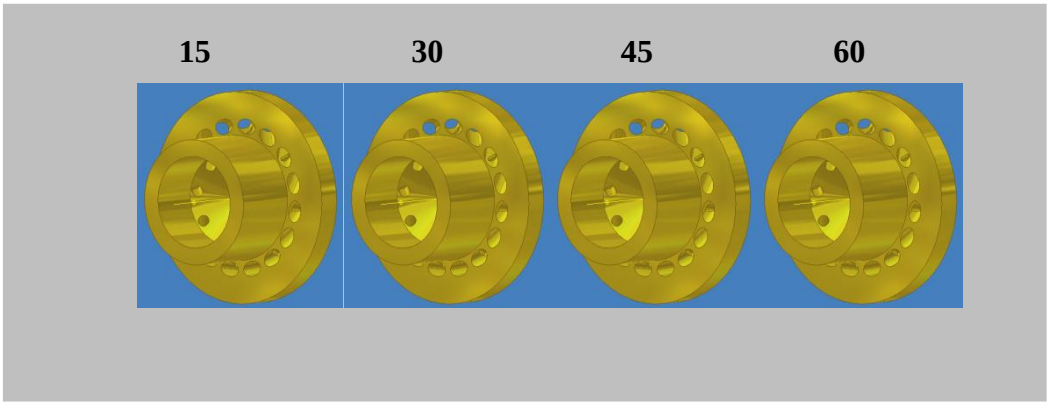

Fig. 7 Injection swirl angles

5. Results and Discussion

The overall structure of the gas flow field can be mainly divided into three regions: a central toroidal recirculation zone (CTRZ), caused by the adverse pressure gradient induced by the swirl, a corner recirculation zone (CRZ), due to the air stream radial expansion and the wall confinement; and a dual shear layer (inner layer around the CTRZ and the outer layer around the CTZ). Both recirculation zones entrain smaller droplets and hot chemically active combustion species from the downstream region of the flame to the root of the flame to improve its stability.
In Fig. 8 these zones are shown through stream vectors by simulation. Results show that with increase of swirl number from 0.2 to 1.73, CTRZ are formed inside the flow. Forward and backward flow which is created by the vortex increase the fuel and air mixing and combustion rate. Moreover, the vortex impact NO_x emissions and create internal FGR in close of the flame.
It can be seen from the Fig 4 that the fuel velocity is high because of the low input diameter. This would create a high flow velocity which moves toward the end of the combustor. Fig 5 shows the temperature contours for some swirl number at equivalence ratio of 1.0. As it is demonstrated, for the low swirl number high temperature region would be found at the end of the combustor. The results show that the region of the maximum flame temperature is tended to the inlet of combustor with increase of swirl number. Furthermore, the temperature is declined with increase of swirl number from 0.2 to 1.73 which has great impact on NO_x exponentially.

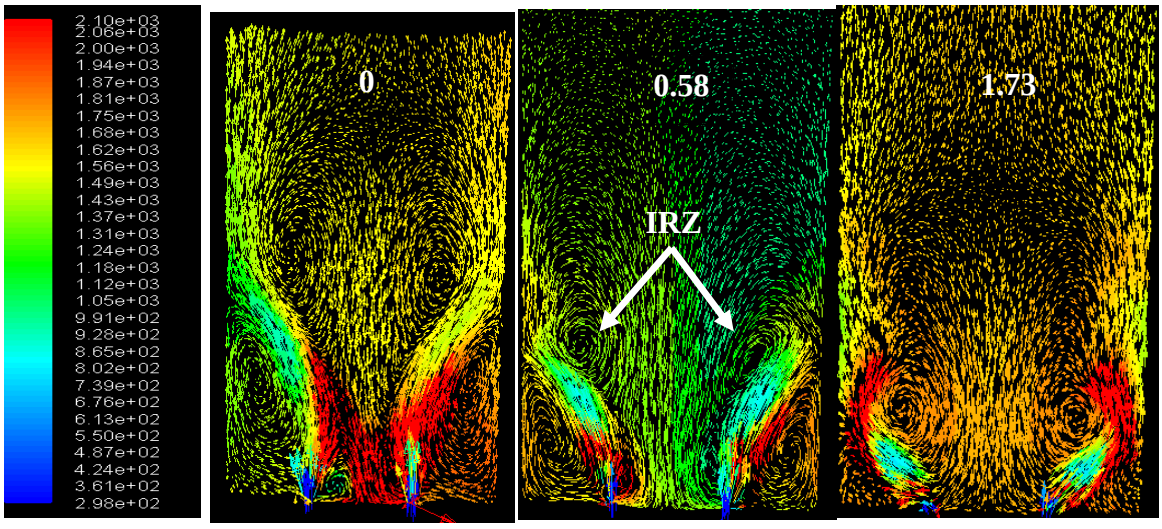

Fig. 8 Flow vectors for various swirl numbers

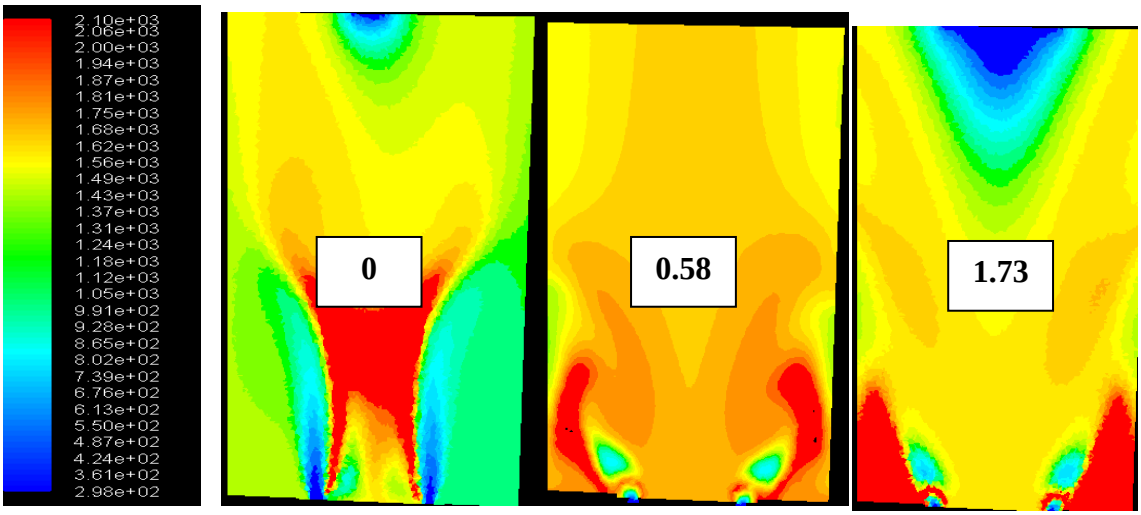

Fig. 9 Temperature contour for swirl number 0, 0.58 and 1.73 and Equivalence ratio of 1.5

For further comparison and validation of current theoretical models, the radial temperature profiles are shown in Figure 10. The maximum predicted flame temperature is 1730 C° which is 110 C° lower than the experimental peak value, good agreement between the numerical and simulation results.

Due to the shortening of the flame length as a result of increasing the injection swirl number (ISN) as mentioned before, the temperature contours become denser and the temperature drops outwards quickly, resulting in steep temperature gradients in Zones 2 and 3 which is clearly indicated in Figure 11.

For both the free and confined CAFB, a three profiles at Z = 20 and 30 mm are smoothly flat and close to each other in the near-centerline region, indicating a uniform temperature distribution in the IRZ in the new burner CAFB. Furthermore, from these two levels which reflect the temperature of the IRZ The temperature contours CAFB burner operating at Re= 6000 and Φ = 1.5 are shown and comparing numerically in Figure 12. It clearly shows that for confined conditions, there is high temperature level in the center of the flame, with a variation

of less than 400 C° in a large region which extends to around Z = 60 mm, this finding is previously verified by flow visualization to be the IRZ.
The highest temperature at the flame front is evidence that most intensive exothermic chemical reactions lies thereunto, i.e. at the edge of the IRZ. This is consistent with Schmittel et al. 2000, which states that the highest temperature is obtained at the boundary of the IRZ and in the IRZ where mainly combustion products prevail, a low heat loss leads to higher temperatures. In the flame boundary outside of the IRZ and especially outside of the flame front, the temperature contours are dense and illustrates that the temperature drops outwards quickly, resulting in steep temperature gradients in Zones 2 and 3.

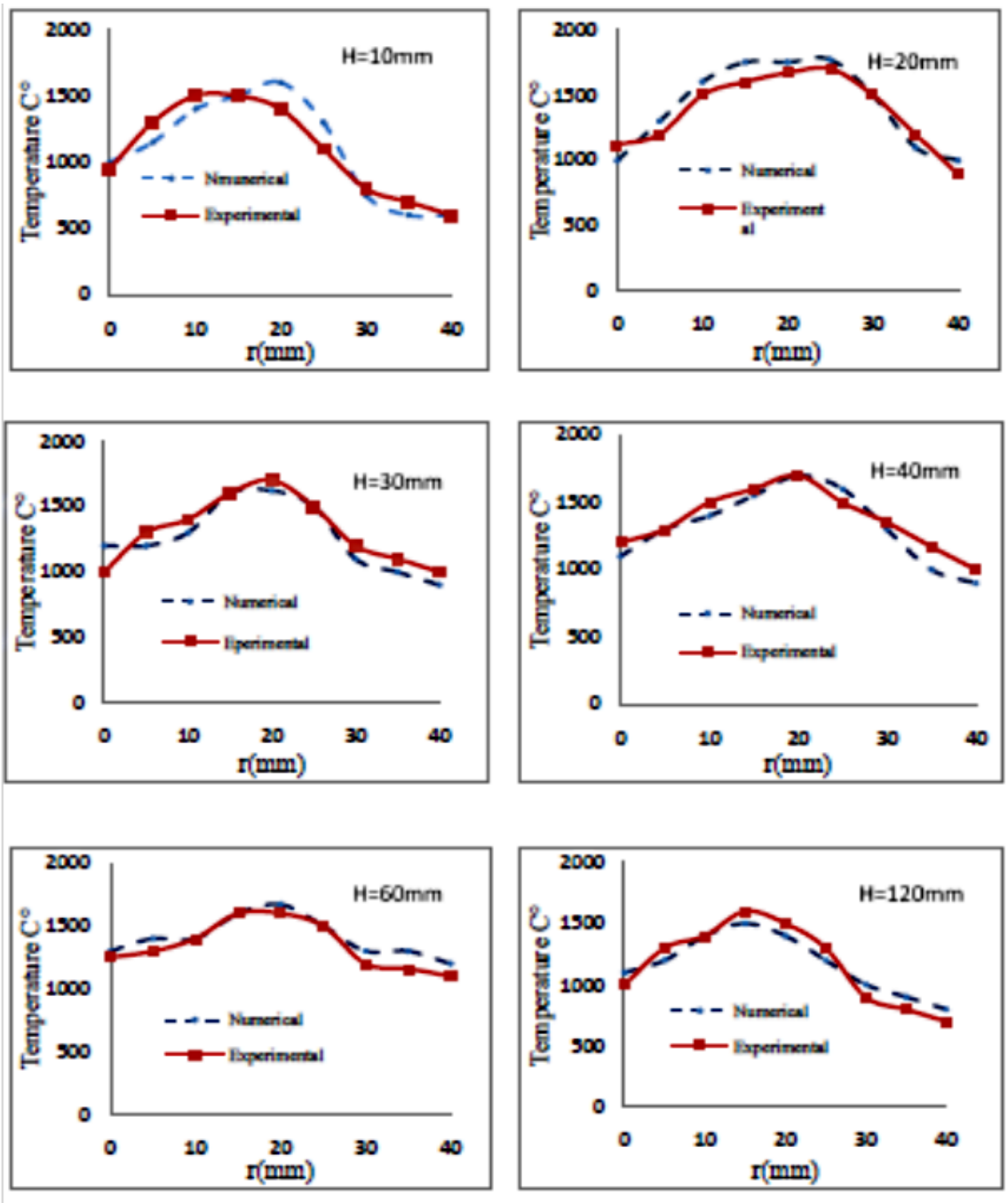

Fig. 10 Comparison of calculated and measured radial temperature profiles of the new burner CAFB at Re= 4000 and Φ =1.5, confined jet

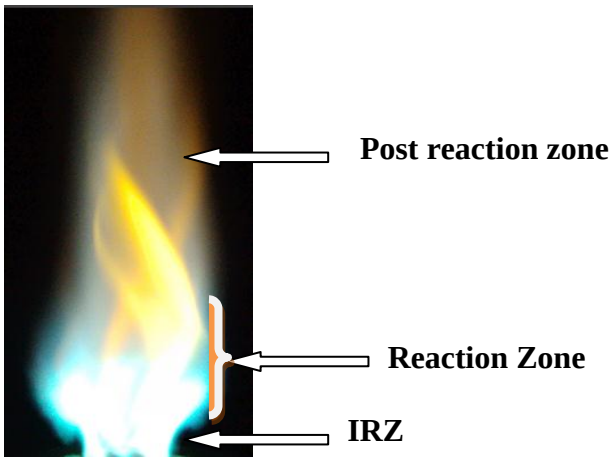

Fig. 11 Experimental flow structures.

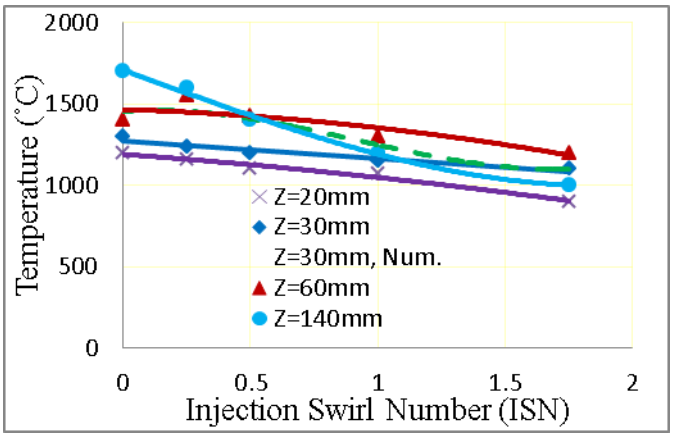

Fig. 12 Flow vectors for various swirl numbers

As previously mentioned the IRZ is quite large and occupies the majority of the flame zone. Therefore, the combustion condition in the IRZ can be considered to be representative of the combustion condition of the entire flame. The low flame temperature results from an overall stoichiometric combustion condition. So, it is an additional justification that CAFB generates a better mixing between fuel and air and leads overall stoichiometric combustion to occur at a higher Φ at certain mass flow rates and with $\Phi = 1.5$.

Figure 13 illustrates the effect of injection swirl number (ISN) on the nitrogen oxide (NO_x) distribution for the new burner CAFB compared to a free jet diffusion flame which is surrounding by a shroud of swirled air, Han Seo Kim 2003 as shown in Figure 12. The two burners have the same heat release rate and measured at the same operating conditions. At ISN = 0 (non-swirl) up to 1, the nitrogen oxide (NO_x) concentration decreases with an increase of ISN. It is clear that with increasing ISN, the flame length decreases and the peak temperature occurs at lower elevations. So, the nitrogen oxide (NO_x) concentration has the same trend of the temperature distribution.

Figure 13 shows also that the nitrogen oxide (NO_x) concentration rapidly decreases at a highly rate in the low swirl burner, in which the injection swirl number (ISN) < 1, while it is decreases in the new burner CAFB from 110 ppm to 70 ppm with the increase of the injection

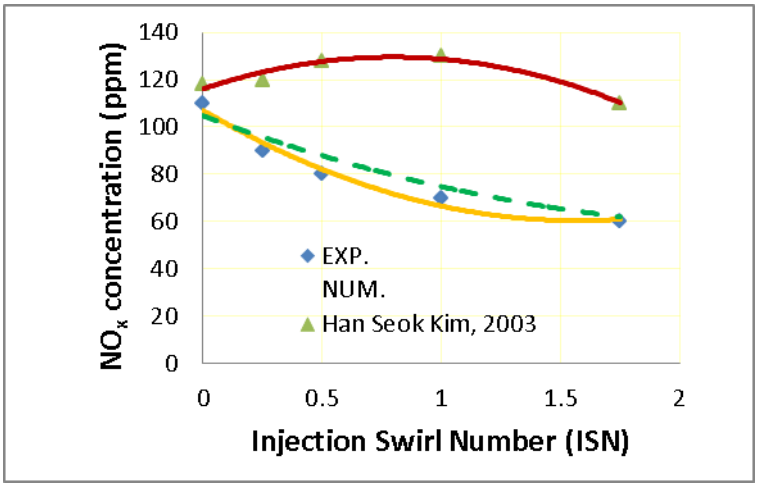

Fig. 13 Flow vectors for various swirl numbers

swirl number (ISN) from 0 to 1.75 in free jet, Han Seo Kim 2003 results indicate that the nitrogen oxide (NO_x) concentration decreases from 120 ppm to 110 ppm , on the other hand it is decrease in confined conditions as shown in Figure 5.41 (b) from 130 to 70 ppm in the new burner CAFB, while decreases in Seaing Wook Baek 2003 from 160 to 70 ppm with the increase of the injection swirl number (ISN) from 0 to 1.75 in the confined conditions. Results indicate that the nitrogen oxide (NO_x) concentrations are lower in the new burner CAFB than the normal swirl burner at flame centerline in confined conditions. Figure 12 shows the compliance between the experimental and numerical results.

Fig. 14 shows NO_x emission for equivalence ratios of 1.5 with various swirl numbers along combustor axis. NO_x is formed at 25 mm from the inlet of combustors where the combustion occurs. NO_x emission is increased with increase of swirl number from 0 to 1.73 then it is declined. As it can be seen from the figures that temperature is affected NO_x emissions.

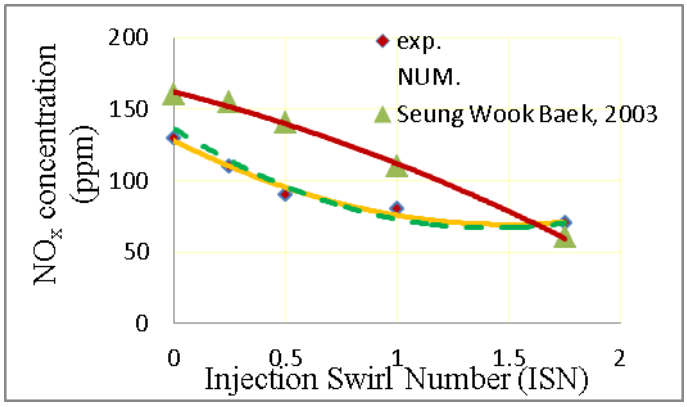

Fig. 14 Flow vectors for various swirl numbers

Figure 14 shows the Numerical and experimental results of the effect of swirl number on NO_x emissions for different equivalence ratios. NO_x is increased with growth of swirl number around 0.2 and then it is declined. The lowest levels of NO_x occurred at swirl number of 1.73. The trend of NO_x emission is similar to temperature which shows the influence of temperature on NO_x. At high swirl number, central toroidal recirculation zone is grown near the combustor wall, so most of the reactants have gone far away from the reaction zone and the combustion temperature and NO_x emission have reduced. The experimental and numerical results are in

good agreement. The results also compared with experimental results of Choi et al.[8] and show good agreement. Fig. 14 shows the experimental results of NO_x emission and temperature at swirl number 1.73 for a range of equivalence ratio. The results show that both temperature and the NO_x emission are increased up to around stoichiometric equivalence ratio and then decreased.

6. Conclusions

The effects of swirl flow on NO_x emission in non premixed flames have been studied numerically and experimentally. It concludes that:

- With use of swirl , flow region is divided to the central toroidal recirculation zone and corner recirculation zone and CTZ
- The maximum flame temperature tends to the inlet of combustor as the swirl number increases.
- The temperature and the levels of NO_x emissions are increased up to swirl number of 0.58 then strongly decreased at the exit of combustor.
- The experimental and numerical results are in good agreement.

7. References

[1] Adi, Surjosatyo, and F. N. Ani. Study of Enhancing the Swirl Burner Performance. International Journal of Engineering & Technology IJET-IJENS Vol: 11 No: 04. , 2011, pp. 21-38.

[2] Brakely, S., Delvosalle, C. and Marlair, G. A two-thermocouples probe for radiation corrections of measured temperatures in compartment fires. Fire Safety British standard. Measurement of Fluid Flow in Closed Conduits. BS 1042: Section 2.1, 1983. Journal, 2003, 39, 399-411.

[3] Beer, J. M. Third International Conference on Combustion and Technology for a Clean Environment, Lisbon, (1995).

[4] Syred N., Progress in Energy and Combustion Systems, Vol. 32, no. 2, (2006) 93-161.

[5] Gupta A.K., Lilley D.J., Syred N., Swirl Flows, Abacus Press, Tunbridge Wells, United Kingdom. (1984).

[6] L. X. Zhou, X. L. Chen And J. Zhang, Proceedings of the Combustion Institute, Volume 29, (2002) 2235-2242.

[7] Zhichao Chen, Zhengqi Li , Jianping Jing, Lizhe Chen, Shaohua Wu, Yang Yao, Energy Conversion and Management 50,(2009) 1180– 1191.

[8] Choeng Ryul Choi a, Chang Nyung Kim, Fuel 88, (2009).

[9] Kurose R, Ikeda M, Makino H, Kimoto M, Miyazaki T, Fuel 83, (2004) 1777–1785.

[10] Lei Peng, Jian Zhang, Chemical Engineering Science 160, (2009) 2903 – 2914.

[11] C. A. Doglas, M.S., Lee, D.S. and Chung, S.H. Effect of swirl on lifted flame characteristics in nonpremixed jets. Combustion and Flame, 2006, 117, 636-645.

[12] Dong, L.L., Cheung, C.S. and Leung, C.W. Heat transfer characteristics of an impinging inverse diffusion flame jet – Part I: Free flame structure. International Journal of Heat and Mass Transfer, 2007, 50, 5108-5123.

[13] Huang, X.Q., Leung, C.W., Chan, C.K. and Probert, S.D. Thermal characteristics of a premixed impinging circular laminar-flame jet with induced swirl. Applied Energy, 2006, 83, 401-411.

[14] Versteeg, H. K. and Malaseke, W., Longman Scientific & Technical, (1996).

[15] FLUENT. Fluent Inc., Fluent 6.3.26 User Manual, 2007.

[16] Ji-Hyun Kwark, Yong-Ki Jeong, Chung-Hwan Jeon, and Young-June Chang, Flow, Turbulence and Combustion 73, (2004) 231–257.